Neural correlates of working memory and its association with metabolic parameters in early-treated adults with phenylketonuria

Stephanie Abgottspon [a,b,f], Raphaela Muri [a,b,c,f], Shawn E. Christ [d], Michel Hochuli [a], Piotr Radojewski [c,f], Roman Trepp [a,f,1], Regula Everts [a,e,f,1,*]

[a] Department of Diabetes, Endocrinology, Nutritional Medicine and Metabolism, Inselspital, Bern University Hospital and University of Bern, Switzerland
[b] Graduate School for Health Sciences, University of Bern, Switzerland
[c] Support Center for Advanced Neuroimaging (SCAN), Institute of Diagnostic and Interventional Neuroradiology, Inselspital, Bern University Hospital and University of Bern, Switzerland
[d] Department of Psychological Sciences, University of Missouri, Columbia, MO, USA
[e] Division of Neuropaediatrics, Development and Rehabilitation, Inselspital Bern, Children's University Hospital, Bern, Switzerland
[f] Translational Imaging Center (TIC), Swiss Institute for Translational and Entrepreneurial Medicine, Bern, Switzerland

ARTICLE INFO

ABSTRACT

Background: Phenylketonuria (PKU) is an inborn error of metabolism affecting the conversion of phenylalanine (Phe) into tyrosine. Previous research has found cognitive and functional brain alterations in individuals with PKU even if treated early. However, little is known about working memory processing and its association with task performance and metabolic parameters. The aim of the present study was to examine neural correlates of working memory and its association with metabolic parameters in early-treated adults with PKU.
Methods: This cross-sectional study included 20 early-treated adults with PKU (mean age: 31.4 years ± 9.0) and 40 healthy controls with comparable age, sex, and education (mean age: 29.8 years ± 8.2). All participants underwent functional magnetic resonance imaging (fMRI) of working memory to evaluate the fronto-parietal working memory network. Fasting blood samples were collected from the individuals with PKU to acquire a concurrent plasma amino acid profile, and retrospective Phe concentrations were obtained to estimate an index of dietary control.
Results: On a cognitive level, early-treated adults with PKU displayed significantly lower accuracy but comparable reaction time in the working memory task compared to the control group. Whole-brain analyses did not reveal differences in working memory-related neural activation between the groups. Exploratory region-of-interest (ROI) analyses indicated reduced neural activation in the left and right middle frontal gyri and the right superior frontal gyrus in the PKU group compared to the control group. However, none of the ROI analyses survived correction for multiple comparisons. Neural activation was related to concurrent Phe, tyrosine, and tryptophan concentrations but not to retrospective Phe concentrations.
Conclusion: In early-treated adults with PKU, cognitive performance and neural activation are slightly altered, a result that is partly related to metabolic parameters. This study offers a rare insight into the complex interplay between metabolic parameters, neural activation, and cognitive performance in a sample of individuals with PKU.

1. Introduction

Phenylketonuria (PKU) is an autosomal recessive inborn error of metabolism characterized by a mutation in the phenylalanine hydroxylase gene resulting in reduced enzyme activity (Blau et al., 2010). Impaired conversion of phenylalanine (Phe) into tyrosine leads to Phe accumulation in the blood and brain (Blau et al., 2010). High Phe concentrations during childhood have a severe adverse effect on

cognitive and neurological development (Blau et al., 2010; De Groot et al., 2010). Therefore, to control Phe levels and prevent adverse long-term outcomes, a restriction of natural protein intake and supplementation with a Phe-free amino acid mixture is initiated immediately after diagnosis of PKU during newborn screening.

The early-initiated treatment leading to the successful prevention of profound mental retardation was a huge medical success in the care of patients with PKU (Van Wegberg et al., 2017). However, slight alterations in cognitive performance can still be observed in individuals with early-treated PKU. More specifically, although most early-treated adults with PKU perform within the normal range, as a group, their cognitive performance was significantly lower than that of a control group (Romani et al., 2019). The cognitive domains reported to be most affected by early-treated PKU are working memory (Aitkenhead et al., 2021; Ashe et al., 2019; Christ et al., 2010a; Hofman et al., 2018), inhibitory control (Jahja et al., 2017; Sundermann et al., 2020), IQ (Feldmann et al., 2019; Jahja et al., 2017; Palermo et al., 2017), processing speed (Aitkenhead et al., 2021; Palermo et al., 2017), and attention (Hofman et al., 2018; Jahja et al., 2017; Palermo et al., 2017). In terms of working memory, age-related changes in performance have been suggested with reduced working memory performance in later childhood but not in earlier childhood compared to a control group (White et al., 2002). Conversely, other studies have reported intact working memory performance (Bilder et al., 2016), inhibitory control (Palermo et al., 2017; Sundermann et al., 2011), and processing speed (Bartus et al., 2018). These findings indicate that developmental trajectories of working memory might be altered and highlight the importance of investigating working memory in early-treated adults with PKU (White et al., 2002).

Functional magnetic resonance imaging (fMRI) provides insights into functional brain organization in individuals with early-treated PKU. Altered neural activation of the working memory network (Christ et al., 2013) and reduced functional connectivity within prefrontal areas (Christ et al., 2010b) was found in individuals with early-treated PKU when performing a working memory task. The fronto-parietal working memory network refers to a set of brain regions that are activated while the participants perform a working memory task (Mencarelli et al., 2019). However, the involved regions in this network are not specific to working memory processing; there is a substantial neural overlap of fronto-parietal regions with other higher-order cognitive domains, such as inhibition, cognitive flexibility, planning, or cognitive control (Niendam et al., 2012). Investigating the neural basis of inhibitory control, little or no difference was found in terms of neural activation between early-treated individuals with PKU and a control group (Sundermann et al., 2020; Sundermann et al., 2011). Furthermore, evidence from task-based and resting-state fMRI suggests increased activation (Sundermann et al., 2020) and lower functional brain connectivity in the default mode network (DMN) in individuals with early-treated PKU (Christ et al., 2012). However, studies using fMRI in early-treated PKU are limited, and small sample sizes and heterogeneous participant characteristics remain a limitation.

Pathophysiological mechanisms of cognitive and neural alterations in individuals with PKU are still not well understood (Berguig et al., 2019; Guerra et al., 2020; Hofman et al., 2018). One hypothesis is that Phe and other large neutral amino acids (LNAA), such as tyrosine and tryptophan, compete for the same transporter (LAT1) across the blood–brain barrier (De Groot et al., 2010; Hofman et al., 2018). Due to higher Phe concentrations in individuals with PKU, the LAT1 transporter is saturated by Phe, resulting in a shortage of LNAA in the central nervous system (Van Spronsen et al., 2009). Tryptophan is a precursor of serotonin, whereas tyrosine is a precursor of dopamine and noradrenaline (Blau et al., 2010; Boot et al., 2017; Surtees & Blau, 2000). Working memory performance, however, relies on an intact prefrontal cortex and dopaminergic activity: A possible disruption in cerebral protein synthesis due to reduced availability of non-Phe LNAA may lead to cognitive disturbances (Christ et al., 2010a; De Groot et al., 2010; Ott & Nieder, 2019). Normalization of LNAA concentration in the central nervous system in addition to the prevention of high Phe concentrations is hypothesized to be essential to avoid PKU-related effects on cognitive functions (Van Spronsen et al., 2009).

Differences in the vulnerability of the brain to Phe likely contribute to the variability in adult cognitive performance (Nardecchia et al., 2015; van Vliet et al., 2019). Phe levels alone do not fully explain the range of cognitive outcomes as some adults achieve a good outcome despite higher Phe levels during childhood, adolescence, or adulthood (Nardecchia et al., 2015; Van Vliet et al., 2018; 2019). For instance, Waisbren et al. (2016) suggested that both high cerebral Phe and low cerebral tyrosine were related to poorer cognitive performance in nine early-treated adults with PKU. Investigating the factors that affect the outcome beyond high Phe levels is thus essential in understanding the underlying pathology and improving patients' care and well-being (Scala et al., 2020; Van Spronsen et al., 2009).

The aim of the present study was to examine working memory performance and related neural activation in early-treated adults with PKU. More specifically, we aimed to investigate whether individuals with early-treated PKU displayed altered activation patterns in the fronto-parietal working memory network compared to a control group. We further explored the interrelationship between neural activation, task performance, and concurrent as well as retrospective metabolic parameters.

2. Materials and methods

2.1. Participants

This cross-sectional study used data from the PICO research program, an ongoing clinical trial at the Department of Diabetes, Endocrinology, Nutritional Medicine and Metabolism of the University Hospital of Bern, Switzerland (Trepp et al., 2020). The PICO study was approved by the local ethics committee of Bern, registered on clinicaltrials.gov (NCT03788343), and conducted in accordance with the Declaration of Helsinki. All participants gave written informed consent prior to participation.

Individuals with PKU were recruited through their metabolic specialist at the University Hospital of Bern, Zurich, or Lausanne. Study visits took place at the Department of Diabetes, Endocrinology, Nutritional Medicine and Metabolism, University Hospital of Bern. Inclusion criteria for the PKU group were a diagnosis of classical PKU after a positive newborn screening, initiation of the Phe-restricted diet within the first 30 days of life, and age ≥ 18 years. Individuals with PKU were excluded if they (i) did not follow a Phe-restricted diet during the six months before the study; (ii) exhibited Phe concentrations > 1600 μmol/L during the six months before the study; (iii) had concomitant diseases influencing the study outcomes (untreated vitamin B12 deficiency); (iv) were pregnant, lactating, or planned a pregnancy; (v) displayed conditions that interfere with the MRI acquisition; (vi) were treated with sapropterin dihydrochloride (Kuvan®) or pegvaliase (Palynziq®). Forty-five individuals with PKU were assessed for eligibility up to the end of March 2021. Nine of them did not meet the inclusion criteria, 11 declined to participate, and four individuals were non-responders, resulting in a sample of 21 early-treated adults with PKU. One individual with PKU was subsequently excluded because of excessive head motion during the fMRI acquisition (see 2.4.3. fMRI preprocessing and analysis).

An age, sex, and education comparable control group was recruited through advertisements on the hospital homepage and flyers distributed within the community. Inclusion criteria for the healthy control group were age ≥ 18 years and no conditions that interfered with the MRI acquisition. None of the participants (PKU nor control group) used psychoactive medications (e.g., SSRIs or stimulants) at the time of study participation.

2.2. Baseline and metabolic data

Socioeconomic status and IQ were included in the baseline data. IQ was estimated with a short form of the WAIS-IV using the four subtests matrix reasoning, symbol search, vocabulary, and arithmetic (Van Ool et al., 2017; Petermann, 2012). The highest level of education was used as a proxy for socioeconomic status. For the PKU group only, blood sampling was performed between 6:30 and 8:00 am after an 8–12-hour overnight fast. Plasma amino acid profiles were measured on a Biochrom 30 (Saturn & Venus) amino acid analyzer, by high-performance ion-exchange liquid chromatography with post-column photometric detection of ninhydrin-derivatized amino acids, according to the routine procedures of the Laboratory of Clinical Chemistry at the Center for Laboratory Medicine of the University Hospital Bern. Concurrent Phe, tyrosine, and tryptophan were recorded in the present study.

Most of the individuals with PKU had collected dry blood spots regularly since diagnosis or gave plasma to check their Phe values. Retrospective Phe values were compiled from medical records and the newborn screening lab in Zurich. Because the availability of retrospective Phe values varied between and within participants, we calculated the median Phe concentrations for each 12-month period (Aitkenhead et al., 2021; Jahja et al., 2017). The medians of the 12-month period were averaged to estimate the index of dietary control (IDC) in three age bands: childhood (0–12 years), adolescence (13–17 years), and adulthood (18 years–present). Both plasma and dry blood spots were included. We did not use a calibration factor for dry blood spots because of the large variability across participants and changes in analytical methods during the past few decades (Stroup et al., 2016).

A total of 4,118 observations were collected. Of these, 122 observations indicated that the Phe value was < 100 μmol/l with no exact value available. Since excluding these observations would bias the sample, we replaced those values with the median of all Phe values lower than 100 μmol/l ($n = 180$, median = 50 μmol/l). In addition, Phe concentrations noted as ranges were centered (e.g., 200–400 μmol/l = 300 μmol/l). If more than three 12-month periods per age band were missing, the participant was excluded from the analysis of the relevant IDC. For two of the 20 individuals with PKU, no information about retrospective Phe values was available.

2.3. Statistical analysis

Statistical analyses of baseline and fMRI task performance were performed with IBM SPSS Statistics, version 25.0. Data visualization was conducted using Graphpad Prism, version 9 (GraphPad Software, San Diego, CA, USA). Categorical variables are displayed as frequencies and percentages and continuous variables as mean and standard deviation. Baseline data were compared between the two groups using a two-tailed χ^2 test or a two-tailed Mann-Whitney U test. Differences in fMRI task performance were computed with a series of analyses of covariance (ANCOVA) with age as a covariate. Partial eta squared (η_p^2) was reported as effect size for ANCOVAs ($\eta_p^2 = 0.01$ indicates a small effect, $\eta_p^2 = 0.06$ indicates a medium effect, $\eta_p^2 = 0.14$ indicates a large effect (Cohen, 1988). Associations between working memory performance and metabolic parameters were examined using two-sided non-parametric partial correlations adjusted for the effect of age. Effect sizes (r_s) were interpreted as follows: $r_s = 0.10$ small effect, $r_s = 0.30$ medium effect, $r_s = 0.50$ large effect (Cohen, 1988). All p-values < 0.05 were considered statistically significant.

2.4. Neuroimaging

2.4.1. fMRI task

Participants completed a visuo-spatial working memory task (n-back, adapted from Jaeggi et al., 2010) with two conditions: 1-back (a control condition with little or no working memory requirements) and 3-back (a condition with high working memory requirements) in a block

design (Fig. 1). During the 1-back condition, participants decided whether a square matched the spatial position of the square presented one stimulus before. During the 3-back condition, participants were asked to determine whether a square was in the same position as the square presented three stimuli before. The squares were presented in one of the eight possible spatial positions, and a white fixation cross was displayed in the center of the black screen. Using their dominant hand, participants pressed a response button (only targets required a response). To familiarize participants with the task, they all practiced it before the MRI session began.

The entire task lasted 9 min and 42 sec with a total of eight task blocks (four per condition) in alternating order, beginning with a 1-back block. Each block lasted 60 sec with 20 stimuli, six of which were targets. The location and sequence of the stimuli were pseudo-randomized. Stimuli were presented for 500 ms with an inter-stimulus interval of 2500 ms. Prior to each block, an instruction screen indicating the condition (1-back or 3-back) appeared for six seconds, followed by a fixation cross for six seconds. After the last block, a fixation cross appeared for 12 sec allowing the BOLD signal to recover. Responses were recorded as true positive (TP), true negative (TN), false positive (FP), and false negative (FN). Accuracy was calculated as follows: $\left(\frac{TP+TN}{TP+TN+FP+FN}\right)*100$ (Zhu et al., 2010). In addition, reaction time was recorded for each participant. The task was completed with the participants in a fasting state.

2.4.2. fMRI data acquisition

fMRI data were obtained on a 3-Tesla Siemens Magnetom Prisma whole-body scanner (Siemens Erlangen, Germany) equipped with a gradient system and a 64-channel head coil. Functional images were acquired using multi-slice single-shot T2-weighted echo-planar imaging with the following parameters: repetition time (TR) = 1000 ms, echo time (TE) = 30 ms, acquisition time (TA) = 9:52 min, flip angle (FA) = 80°, field-of-view (FOV) = 192 × 192 mm, 48 slices in interleaved ascending acquisition order and a slice thickness of 2 mm; a total of 582 images were recorded. Anatomical T1-weighted images were acquired using a magnetization-prepared rapid acquisition gradient-echo (MP-RAGE) sequence (TR = 1950 ms, TE = 2.26 ms; inversion time (TI) = 900 ms, TA = 4:34 min, FA = 9°, FOV = 256 mm × 256 mm, matrix dimension = 256 × 256, isotropic voxel resolution = 1 mm³; with a total of 176 sagittal slices).

2.4.3. fMRI preprocessing and analysis

fMRI data were preprocessed using the SPM12 software (Wellcome Trust Centre for Neuroimaging, London, UK) implemented in MATLAB R2017b (Mathworks, Natick, MA, USA). We included the following steps in the preprocessing pipeline: (i) all functional images were realigned and resliced to the mean functional image, and a six-parameter rigid body transformation was applied to correct for motion distortion; (ii) the mean functional image was co-registered to the structural image; (iii) the data were segmented and then spatially normalized into the Montreal Neurological Institute (MNI) space with a voxel size of 2 × 2 × 2 mm³; (iv) functional images were smoothed with a Gaussian Kernel of 8 mm full-width at half-maximum (FWHM). To account for residual movement after realignment, we used the artifact detection (ART) toolbox (http://www.nitrc.org/projects/artifact_detect) to detect volume artifacts in the fMRI time series. Volumes with a global mean intensity z-threshold > 5 and a movement threshold > 0.9 mm were considered artifactual. An additional nuisance regressor was entered into the first-level analysis for every volume identified as an outlier according to the ART toolbox. Participants who had > 15% volumes identified as outliers were excluded, resulting in one individual with PKU being excluded. The final study sample consisted of 20 individuals with PKU and 40 controls. In the PKU group, significantly more volumes were identified as outliers due to head motion (28.55 ± 23.24) than in the control group (11.85 ± 17.75; $U = 209.50$, $p = .003$).
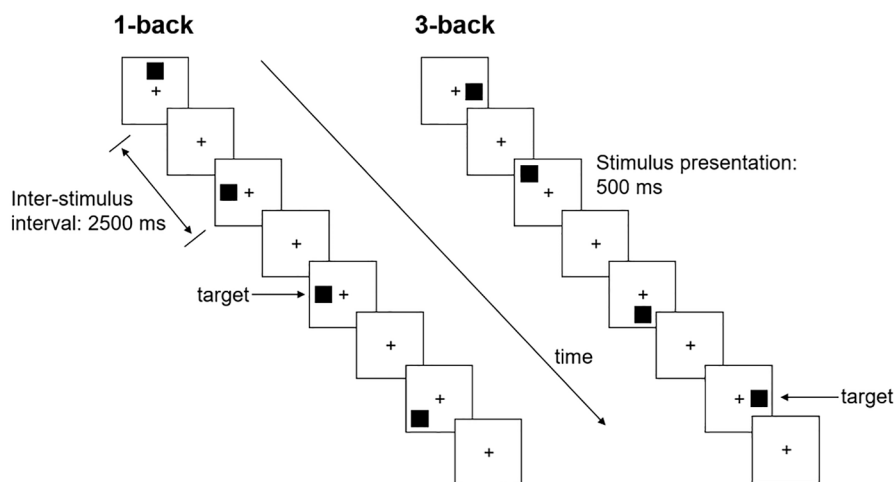
Fig. 1. fMRI working memory task.

The general linear model (GLM) was applied for whole-brain first-level analyses. The six motion parameters from the rigid body realignment and the additional regressors identified by the ART toolbox were entered as nuisance regressors into the GLM. The data were modelled as boxcar function convolved with a canonical hemodynamic response function. A high-pass filter with a cutoff of 128 sec was implemented in the GLM. The relevant contrast image ("3-back > 1-back") was obtained for each participant before being entered into the second-level analyses. One-sample *t*-tests were employed to examine neural activation during working memory performance in both groups separately. Whole-brain between-group differences in the working memory network were analyzed using a two-sample *t*-test. To examine the effects of task performance (accuracy and reaction time for the 3-back condition) and metabolic parameters on neural activation, a series of voxel-wise multiple regressions were performed with neural activation as the dependent variable. Age was entered as a covariate in all neuroimaging analyses to account for age effects on neural activation during working memory processing. The significance level for all voxel-wise analyses was set at $p < .001$ with a minimum extent threshold of 10 voxels. To correct for multiple comparisons, a family-wise error correction (FWE, $p < .05$) was applied at the cluster level. Per default, SPM implements random field theory to define the critical threshold for cluster-based inference (Ostwald et al., 2019).

To corroborate whole-brain analyses, exploratory region-of-interest (ROI) analyses were run. Independently defined ROIs were derived from the NeuroSynth database (https://www.neurosynth.org/) (Yarkoni et al., 2011). We searched with the term "working memory" and obtained an association map of 1091 studies included in the automated meta-analysis (threshold z = 3.7). Eighty-five clusters were identified from the NeuroSynth database. Most of these clusters were very small, with a cluster size not exceeding ten voxels. To limit the number of ROIs, we only included clusters $\geq$ 100 voxels and excluded clusters in the

cerebellum, resulting in nine ROIs for further analysis. ROIs are displayed in Fig. 2 and supplementary Table 1. Parameter estimates (betas) of the contrast 3-back > 1-back were extracted for all participants using

Table 1
Baseline and metabolic data.

	PKU group (n = 20)	Control group (n = 40)	χ2 / U
Baseline data			
Age, years	31.4 ± 9.0	29.8 ± 8.2	345.00
Sex, males, n (%)	10 (50.0)	20 (50.0)	0.000
IQ	97.0 ± 11.9	105.1 ± 13.7	263.00*
SES, n (%)			
High school	0	1 (2.5)	
College/job training	18 (90.0)	34 (85.0)	0.610
Graduate school	2 (10.0)	5 (12.5)	
Metabolic data (μmol/l)			
Plasma Phe	702.6 ± 203.3	–	–
range	380 – 1160		
Plasma tyrosine	41.1 ± 8.7	–	–
range	28 – 62		
Plasma tryptophan	36.5 ± 8.8	–	–
range	21 – 54		
IDC 0–12 years	270.4 ± 67.7	–	–
range	168.7 – 364.5		
IDC 13–17 years	505.3 ± 159.0	–	–
range	292.0 – 795.7		
IDC ≥ 18 years	628.2 ± 204.2	–	–
range	410.62 – 1052.2		

Note. Unless otherwise stated, data are presented as mean ± SD. *$p < .05$ (two-sided); $\chi 2$ = Chi-square test; U = Mann-Whitney U test; SES = Socioeconomic status; IDC = Index of Dietary Control. IDC 0–12 years available for 11 participants, IDC 13–17 years available for 17 participants, IDC ≥ 18 years available for 14 participants.
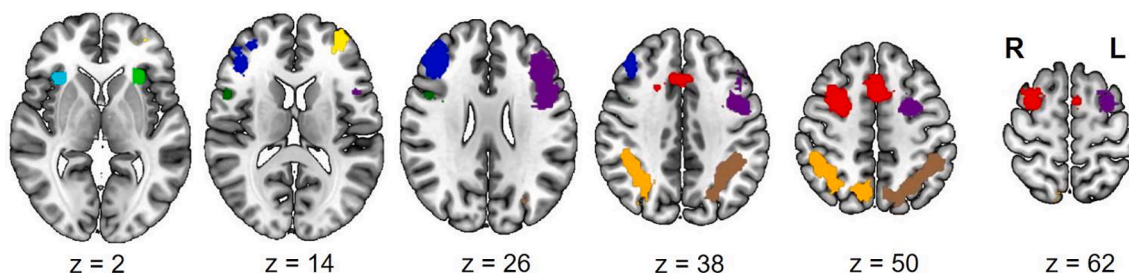

Fig. 2. ROIs derived from the NeuroSynth database.

MarsBar (Brett et al., 2002) and analyzed in SPSS. A series of ANCOVAs (with age as a covariate) were computed to examine whether the two groups differed in their task-related neural activation.

The Automated Anatomical Labeling atlas (aal) was utilized to identify anatomical regions of MNI coordinates (Tzourio-Mazoyer et al., 2002). Visualization of all statistical maps was performed with MRIcroGL using the MNI 152 template (http://www.mccauslandcenter.sc.edu/mricrogl/).

3. Results

3.1. Baseline and metabolic data

Demographic and clinical data are presented in Table 1. The two groups were comparable in terms of age, education, and sex. Mean IQ was within the normal range in both groups but was significantly lower in the PKU group than in the control group ($U = 263.00$, $p = .031$). Eight of 20 individuals with PKU (40%) had concurrent plasma Phe concentrations within the suggested target range (120–600 μmol/l), and 12 of them (60%) showed higher Phe concentrations than suggested by the current European guidelines (Van Wegberg et al., 2017). Concurrent tyrosine concentrations were toward the lower end of the reference range, and 11 individuals with PKU (55%) had concentrations below the reference range of 40–100 μmol/l. The same pattern was observed for tryptophan concentrations: four individuals with PKU (20%) had concentrations below the reference range of 30–90 μmol/l. Phe concentrations were not significantly related to tyrosine ($r_s = 0.143$, $p = .559$) nor to tryptophan concentrations ($r_s = -0.097$, $p = .692$). No significant association was found between tyrosine and tryptophan concentrations ($r_s = -0.002$, $p = .995$).

3.2. fMRI task performance

fMRI task performance was not available for one individual with PKU because of technical problems during the fMRI scanning. Accuracy in the 1-back condition was significantly higher in the control group (98.9% ± 2.1) than in the PKU group (95.3% ± 6.9; ($F(1,56) = 8.237$, $p = .006$, $\eta_p^2 = 0.128$) with a medium effect size. Mean reaction time in the 1-back condition was 525.7 ms ± 147.8 in the control group and 636.3 ms ± 252.5 in the PKU group, which was not significantly different ($F(1,56) = 3.763$, $p = .057$, $\eta_p^2 = 0.063$). A similar pattern was observed for the 3-back condition. Accuracy in the 3-back condition was significantly higher in the control group (87.4% ± 7.9) than in the PKU group (81.4% ± 6.3; $F(1,56) = 7.541$, $p = .008$, $\eta_p^2 = 0.119$) with a medium effect size. Mean reaction time in the 3-back condition was 771.6 ms ± 282.4 in the control group and 816.0 ms ± 306.5 in the PKU group, which was not significantly different ($F(1,56) = 0.168$, $p = .684$, $\eta_p^2 = 0.003$). We used accuracy and reaction time in the 3-back condition for further analyses, as our primary interest was working memory performance.

Subgroup analyses of PKU participants with values above and below the suggested Phe cutoff of 600 μmol/l (current guidelines) found no significant differences in 3-back accuracy ($F(1,16) = 0.967$, $p = .340$, $\eta_p^2 = 0.057$) or reaction time ($F(1,16) = 1.297$, $p = .272$, $\eta_p^2 = 0.075$). There was no significant association between fMRI task performance and concurrent metabolic parameters such as Phe, tyrosine, and tryptophan (supplementary Table 2). Although not statistically significant, a medium effect size was observed for the partial correlation between tyrosine and 3-back reaction time, indicating that faster reaction time was achieved when tyrosine was higher ($r_s = -0.334$, $p = .176$). Retrospective Phe values, indicated by the IDC in different age bands, were unrelated to fMRI task performance.

3.3. Neuroimaging data

3.3.1. Within-group analyses

Results of the within-group whole-brain analyses (one-sample *t*-test)

for the control group are displayed in Table 2. In the control group, significant working memory-related activation was found in the left middle frontal gyrus, right superior and inferior frontal gyri, left precuneus, left insula, and cerebellum. These areas were previously identified as being involved in working memory processing (Owen et al., 2005). In the PKU group, whole-brain analyses revealed no significant activation cluster. Thus, we performed exploratory analyses with small volume correction (SVC) for the PKU group and found task-related neural activation in the left middle frontal gyrus. The ROIs defined based on the NeuroSynth database were used for SVC.

3.3.2. Between-group analyses

Between-group analyses showed no significant differences in neural activation on a whole-brain level. Next, we performed exploratory ROI analyses and extracted the parameter estimates (betas) from the nine ROIs defined by the NeuroSynth database from the contrast 3-back > 1-back. A series of ANCOVAs controlling for the effect of age revealed that the PKU group displayed lower activation than the control group in the left ($F(1,57) = 5.685$, $p = .020$, $\eta_p^2 = 0.091$) and right middle frontal gyri ($F(1,57) = 6.070$, $p = .017$, $\eta_p^2 = 0.096$) and in the right superior frontal gyrus ($F(1,57) = 6.990$, $p = .011$, $\eta_p^2 = 0.109$) with medium effect sizes. Results of the ANCOVA analyses are presented in Fig. 3. After correction for multiple comparisons (FDR correction), no between-group differences remained significant. However, non-corrected results provide additional insight into neural activation and are thus presented in this study. Looking at the whole working memory network (combining the 9 ROIs), no significant differences in terms of neural activation were observed between the two groups ($F(1,57) = 2.524$, $p = .118$, $\eta_p^2 = 0.042$).

3.4. Neural activation and its relation to task performance

Voxel-wise whole-brain multiple regression analyses revealed that fMRI task performance (accuracy and reaction time of the 3-back condition) was not associated with neural activation in the control group or the PKU group.

3.5. Neural activation and its relation to metabolic parameters

In the PKU group, multiple regression analyses revealed that Phe concentrations were negatively related to neural activation in the right middle frontal gyrus (MNI = [34 58 8], $k_E = 176$, $p_{FWE} = 0.044$). Tyrosine concentrations were negatively associated with activation in the left supplementary motor area (SMA; MNI = [−6 − 12 48], $k_E = 331$,

Table 2

Brain areas involved in working memory processing (within-group analyses).

Group	Brain area	MNI coordinate			Cluster level	
		x	y	z	k_E	p
Control group	L insula	−30	22	0	203	0.039
	R inferior frontal gyrus	40	6	30	203	0.039
	L middle frontal gyrus	−28	8	62	5487	0.000
	L middle frontal gyrus	−36	50	14	576	0.000
	R superior frontal gyrus	26	10	54	2734	0.000
	L precuneus	−8	−66	54	7153	0.000
	L cerebellum	−34	−58	−32	205	0.038
	R cerebellum	32	−60	−30	468	0.001
PKU group[a]	L middle frontal gyrus	−24	4	60	69	0.016

Note. L = left; R = right; MNI = Montreal Neurological Institute; *p* = level of significance (FWE-corrected); k_E = cluster size (voxel size $2 \times 2 \times 2$ mm^3); [a] after small volume correction.
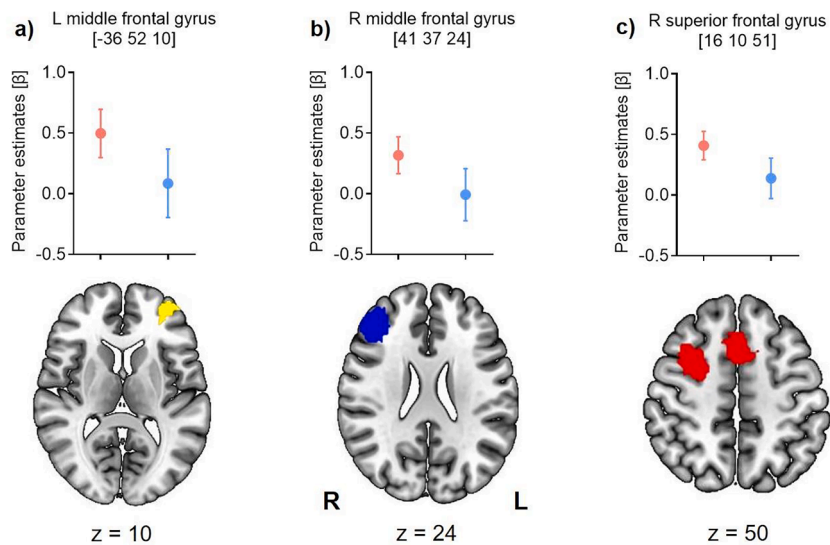
Fig. 3. Parameter extraction of the regions of interest revealed reduced activation in the PKU group in **a)** the left middle frontal gyrus, **b)** the right middle frontal gyrus, and **c)** the right superior frontal gyrus. Estimated marginal means (adjusted for the effect of age) with associated 95% confidence intervals are displayed on the x-axis for the control group (red) and the PKU group (blue). Center of mass MNI coordinates are shown in square brackets. After adjusting for multiple comparisons (FDR correction), no group differences remained significant. L = left; R = right. (For interpretation of the references to colour in this figure legend, the reader is referred to the web version of this article.)

p_{FWE} = 0.002) and the right Rolandic operculum (MNI = [56–12 14], k_E = 255, p_{FWE} = 0.008). There was a significant positive association between tryptophan concentrations and the right middle cingulate gyrus (MNI = [2 8 32], k_E = 210, p_{FWE} = 0.018), left middle temporal gyrus (MNI = [−56 0−20], k_E = 215, p_{FWE} = 0.016), and right middle temporal gyrus (MNI = [44 8−28], k_E = 527, p_{FWE} = 0.000). The results remained the same when estimating a second model with Phe concentrations as covariate (in addition to age). Furthermore, in a subsample of individuals with PKU for whom retrospective Phe levels were available, the IDC in the three age bands did not relate to neural activation. For visualization purposes, we extracted the parameter estimates (β) of the significant clusters and plotted them in relation to the concentration of Phe, tyrosine, or tryptophan, respectively (Fig. 4).

4. Discussion

The present study investigated neural correlates of working memory and its association with metabolic parameters in early-treated adults with PKU. Specifically, we explored whether individuals with PKU displayed altered activation patterns in the fronto-parietal working

memory network compared to a healthy control group. We found that fMRI task accuracy was lower in individuals with PKU, but reaction time was similar to those of the control group. Furthermore, hypoactivation in frontal regions of the working memory network was observed in the PKU group, which, however, did not survive FDR-correction. Finally, concurrent Phe, tyrosine, and tryptophan concentrations were related to neural activation, whereas retrospective Phe concentrations, indicated by the IDC in three age bands, were not.

Working memory performance differed between the PKU group and the control group. More precisely, individuals with PKU displayed significantly reduced task accuracy, although reaction time was comparable, suggesting that they answer as fast but less accurately as the control group. These findings align with previous studies indicating reduced working memory performance in individuals with PKU (Aitkenhead et al., 2021; Ashe et al., 2019; Christ et al., 2010a; Hofman et al., 2018). In addition, IQ was within the normal range but significantly lower in the PKU group compared to the control group, which replicates earlier findings (Feldmann et al., 2019; Jahja et al., 2017; Palermo et al., 2017). It is worth noting that our control group had a mean IQ of 105, which is higher than expected from a normative group.
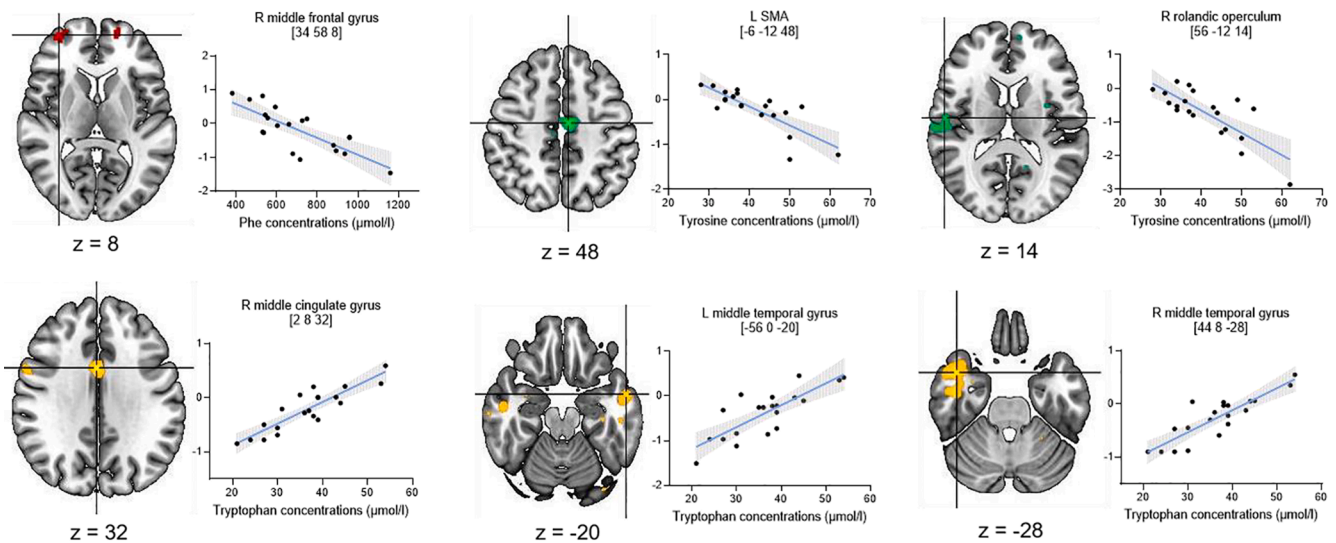

Fig. 4. Parameter extraction of the significant clusters identified in the regression analysis in relation to the metabolic parameters. The blue line represents the fitted line with 95% confidence intervals (shaded area). Parameter estimates (β) on the y-axis. Peak MNI coordinates in brackets. L = left, R = right; SMA = supplementary motor area. (For interpretation of the references to colour in this figure legend, the reader is referred to the web version of this article.)

Hence, our data suggest that the cornerstone in PKU treatment, a Phe-restricted diet and amino acid supplementations, allows early-treated adults with PKU to achieve good performance in terms of working memory and IQ with only subtle alterations.

We observed that individuals with PKU displayed lower activation in frontal regions of the working memory network, namely in the left and right middle frontal gyrus and right superior frontal gyrus. This finding, however, did not survive FDR correction, probably due to the small sample size and correspondingly low statistical power. Our results only partially align with previous studies investigating the neural underpinnings of working memory (Christ et al., 2010b; Christ, Moffitt, Peck, & White, 2013). Adopting a verbal *n*-back design, Christ et al. (2010b, 2013) found widespread activation differences in several ROIs across the frontal, parietal, and temporal lobe; hence not only in areas limited to the frontal lobe such as our findings indicate. However, these earlier studies included individuals with PKU aged from 9 to 33 years, which is substantially different from the more homogeneous sample of adults we present here. Given that age can impact neural activation in the working memory network (Spencer-Smith et al., 2013; Steffener et al., 2009), this might account for the inconsistent findings.

Studies using task-based fMRI to investigate neural activation in adults with PKU are rare. Two previous studies explored the neural basis of inhibitory control using an fMRI Stroop task (Sundermann et al., 2011) or a Go-NoGo task (Sundermann et al., 2020). Compared to a control group, there were either no between-group differences in neural activation of the cognitive control network (Sundermann et al., 2011) or only subtle activation increases in the right middle frontal gyrus in adults with PKU (Sundermann et al., 2020). Differences in neural activation between individuals with PKU and a control group were more pronounced in brain areas outside the cognitive control network (Sundermann et al., 2020). More specifically, increased neural activation was found in several areas of the DMN, such as the middle temporal gyrus or the right posterior cingulate cortex (Sundermann et al., 2020). The DMN is a functional network consisting of multiple cortical areas typically more active at rest than during task performance (Raichle, 2015). Taken together, findings from the studies by Sundermann et al. (2020, 2011) and our results suggest that areas associated with executive functions, such as inhibitory control or, in our case, working memory, are slightly altered in adults with PKU.

In addition, within-group analyses in the PKU group yielded only one significant activation cluster in the left middle frontal gyrus. In contrast, the control group showed widespread activation patterns across the fronto-parietal network. Our fMRI task included a 1-back condition as a control condition. One could speculate that individuals with PKU were already highly engaged in the 1-back condition and required more cognitive resources than the control group. Due to high task engagement in the 1-back condition, the contrast 3-back > 1-back might not yield widespread activation patterns in the PKU group. Also, decreases in fronto-parietal activation may emerge when participants reach their working memory capacity (Lamichhane et al., 2020; Van Snellenberg et al., 2015). This indicates that the 3-back task was cognitively engaging for the PKU group leading only to focal activation of the left middle frontal gyrus rather than activation patterns distributed across the fronto-parietal network.

Our findings suggest that concurrent Phe, tyrosine, and tryptophan concentrations are associated with neural activation. A negative association between neural activation in the right middle frontal gyrus and Phe concentrations was observed. Higher tyrosine concentrations were related to reduced activity in the left SMA and right Rolandic operculum. Additionally, higher tryptophan concentrations were associated with increased activity in the left and right middle temporal gyri and right middle cingulate gyrus, brain areas that do not primarily belong to the fronto-parietal working memory network. The middle temporal gyrus is a central component of the language network (Acheson & Hagoort, 2013), and the SMA is involved in several processes such as the execution of movement sequences and cognitive control (Nachev et al.,

2008). Interestingly, only concurrent but not retrospective Phe values were associated with neural activation. Furthermore, there was a non-significant association with medium effect size between concurrent tyrosine concentrations and 3-back reaction time, suggesting that higher tyrosine levels were related to faster reaction time. This would indicate that amino acid supplementation, the primary source of tyrosine in individuals with PKU, is essential for intact response speed. Our results provide preliminary insights into the association between neural activation, task performance, and metabolic parameters. Additional studies are needed to elucidate the interrelationship between these parameters. In the context of the PICO study, we will investigate whether a four-week intervention with Phe is related to changes in cognitive performance and neural activation (Trepp et al., 2020).

This study is subject to some limitations. First, measurements of metabolic parameters were not available for the control group. Second, data on concurrent and retrospective metabolic parameters should be interpreted with caution. Concurrent metabolic parameters are assessed in the fasting state, and concentrations might rise after amino acid supplementation; thus, we cannot conclude from the fasting data how good the performance would be after the intake of the supplementation. In terms of retrospective Phe values, we collected information to estimate an IDC in three different age bands. However, the IDCs were only available for a subgroup of the participants, and the number of observations varied considerably between and within the participants. Some participants did not monitor their dietary adherence on a regular basis or did not collect dry blood samples when they were not very compliant with their diet, which in turn biases the calculation of an IDC. Third, the present study is a convenience sample, and results have to be interpreted cautiously with regard to the representativeness of the participants and generalizability of the findings. Fourth, the sample size is relatively small. This, however, is often an issue when investigating rare diseases such as PKU, given the prevalence is only 1 per 8,000 newborns in Europe (Loeber, 2007). To reduce heterogeneity, we included only early-treated individuals with classical PKU following a Phe-restricted diet. It remains to be established whether the characteristics examined behave similarly in individuals with only mild PKU.

4.1. Conclusion

Early-treated adults with PKU demonstrated less accurate but comparable reaction time in a working memory task compared to the control group. Further, exploratory ROI analyses suggested reduced neural activation in frontal areas of the working memory network in the PKU group compared to the control group, which, however, did not survive correction for multiple comparisons. Furthermore, concurrent but not retrospective metabolic parameters were related to neural activation in several brain areas. Our results shed light on the complex interplay between concurrent metabolic parameters, in particular tyrosine and tryptophan, neural activation, and cognitive performance. Future studies could combine different imaging modalities such as structural and functional imaging or MR spectroscopy to get a closer insight into how PKU affects the brain and its functions.

CRediT authorship contribution statement

Stephanie Abgottspon: Methodology, Formal analysis, Investigation, Data curation, Writing – original draft, Visualization, Project administration, Funding acquisition. **Raphaela Muri:** Validation, Conceptualization, Investigation, Data curation, Writing – review & editing, Funding acquisition, Project administration. **Shawn E. Christ:** Writing – review & editing. **Michel Hochuli:** Resources, Writing – review & editing. **Piotr Radojewski:** Writing – review & editing. **Roman Trepp:** Conceptualization, Resources, Writing – review & editing, Supervision, Funding acquisition, Project administration. **Regula Everts:** Conceptualization, Resources, Writing – review & editing, Supervision, Funding acquisition, Project administration.

Declaration of Competing Interest

Acknowledgements

Appendix A. Supplementary data

Supplementary data to this article can be found online at https://doi.org/10.1016/j.nicl.2022.102974.

References

Acheson, D.J., Hagoort, P., 2013. Stimulating the Brain's Language Network: Syntactic Ambiguity Resolution after TMS to the Inferior Frontal Gyrus and Middle Temporal Gyrus. J. Cogni. Neurosci. 25 (10), 1664–1677. https://doi.org/10.1162/jocn.

Aitkenhead, L., Krishna, G., Ellerton, C., Moinuddin, M.d., Matcham, J., Shiel, L., Hossain, S., Kiffin, M., Foley, J., Skeath, R., Cleary, M., Lachmann, R., Murphy, E., 2021. Long-term cognitive and psychosocial outcomes in adults with phenylketonuria. J. Inherit. Metab. Dis. 44 (6), 1353–1368. https://doi.org/10.1002/jimd.12413.

Ashe, K., Kelso, W., Farrand, S., Panetta, J., Fazio, T., De Jong, G., Walterfang, M., 2019. Psychiatric and Cognitive Aspects of Phenylketonuria: The Limitations of Diet and Promise of New Treatments. Front. Psychiatry 10, 1–20. https://doi.org/10.3389/fpsyt.2019.00561.

Bartus, A., Palasti, F., Juhasz, E., Kiss, E., Simonova, E., Sumanszki, C., Reismann, P., 2018. The influence of blood phenylalanine levels on neurocognitive function in adult PKU patients. Metab. Brain Dis. 33 (5), 1609–1615. https://doi.org/10.1007/s11011-018-0267-6.

Berguig, G.Y., Martin, N.T., Creer, A.Y., Xie, L., Zhang, L., Murphy, R., Pacheco, G., Bullens, S., Olbertz, J., Weng, H.H., 2019. Of mice and men: Plasma phenylalanine reduction in PKU corrects neurotransmitter pathways in the brain. Mol. Genet. Metab. 128 (4), 422–430. https://doi.org/10.1016/j.ymgme.2019.08.004.

Bilder, D.A., Noel, J.K., Baker, E.R., Irish, W., Chen, Y., Merilainen, M.J., Prasad, S., Winslow, B.J., 2016. Systematic Review and Meta-Analysis of Neuropsychiatric Symptoms and Executive Functioning in Adults With Phenylketonuria Systematic Review and Meta-Analysis of Neuropsychiatric. Dev. Neuropsychol. 41 (4), 245–260. https://doi.org/10.1080/87565641.2016.1243109.

Blau, N., van Spronsen, F.J., Levy, H.L., 2010. Phenylketonuria. The Lancet 376 (9750), 1417–1427. https://doi.org/10.1016/S0140-6736(10)60961-0.

Boot, E., Hollak, C.E.M., Huijbregts, S.C.J., Jahja, R., van Vliet, D., Nederveen, A.J., Nieman, D.H., Bosch, A.M., Bour, L.J., Bakermans, A.J., Abeling, N.G.G.M., Bassett, A.S., van Amelsvoort, T.A.M.J., van Spronsen, F.J., Booij, J., 2017. Cerebral dopamine deficiency, plasma monoamine alterations and neurocognitive de fi cits in adults with phenylketonuria. Psychol. Med. 47 (16), 2854–2865. https://doi.org/10.1017/S0033291717001398.

Brett, M., Anton, J.-L., Valabregue, R., Poline, J., 2002. Region of interest analysis using an SPM toolbox. In *8th International Conference on Functional Mapping of the Human Brain Neuroimage, Sendai, Japan*.

Christ, S.E., Huijbregts, S.C.J., de Sonneville, L.M.J., White, D.A., 2010a. Executive function in early-treated phenylketonuria: Profile and underlying mechanisms. Mol. Genet. Metab. 99, 22–32. https://doi.org/10.1016/j.ymgme.2009.10.007.

Christ, S.E., Moffitt, A.J., Peck, D., 2010b. Disruption of prefrontal function and connectivity in individuals with phenylketonuria. Mol. Genet. Metab. 99, S33–S40. https://doi.org/10.1016/j.ymgme.2009.09.014.

Christ, S.E., Moffitt, A.J., Peck, D., White, D.A., 2013. The effects of tetrahydrobiopterin (BH4) treatment on brain function in individuals with phenylketonuria. NeuroImage: Clinical 3, 539–547. https://doi.org/10.1016/j.nicl.2013.08.012.

Christ, S.E., Moffitt, A.J., Peck, D., White, D.A., Hilgard, J., 2012. Decreased functional brain connectivity in individuals with early-treated phenylketonuria: Evidence from resting state fMRI. J. Inherit. Metab. Dis. 35 (5), 807–816. https://doi.org/10.1007/s10545-011-9439-9.

Cohen, J. (1988). *Statistical Power Analysis for the Behavioral Sciences*.

De Groot, M.J., Hoeksma, M., Blau, N., Reijngoud, D.J., van Spronsen, F.J., 2010. Pathogenesis of cognitive dysfunction in phenylketonuria: Review of hypotheses. Mol. Genet. Metab. 99, S86–S89. https://doi.org/10.1016/j.ymgme.2009.10.016.

Feldmann, R., Osterloh, J., Onon, S., Fromm, J., Rutsch, F., Weglage, J., 2019. Neurocognitive functioning in adults with phenylketonuria: Report of a 10-year follow-up. Mol. Genet. Metab. 126 (3), 246–249. https://doi.org/10.1016/j.ymgme.2018.12.011.

Guerra, I.M.S., Ferreira, H.B., Neves, B., Melo, T., Diogo, L.M., Domingues, M.R., Moreira, A.S.P., 2020. Lipids and phenylketonuria: Current evidences pointed the need for lipidomics studies. Arch. Biochem. Biophys. 688 (March), 108431 https://doi.org/10.1016/j.abb.2020.108431.

Hofman, D.L., Champ, C.L., Lawton, C.L., Henderson, M., Dye, L., 2018. A systematic review of cognitive functioning in early treated adults with phenylketonuria. Orphan. J. Rare Dis. 13 (1), 150. https://doi.org/10.1186/s13023-018-0893-4.

Jaeggi, S.M., Buschkuehl, M., Perrig, W.J., Meier, B., 2010. The concurrent validity of the N-back task as a working memory measure. Memory 18 (4), 394–412. https://doi.org/10.1080/09658211003702171.

Jahja, R., Huijbregts, S.C.J., De Sonneville, L.M.J., van der Meere, J.J., Legemaat, A.M., Bosch, A.M., van Spronsen, F.J., 2017. Cognitive profile and mental healthy in adult phenylketonuria: A PKU-COBESCO study. Neuropsychology 31 (4), 437–447. https://doi.org/10.1037/neu0000358.

Lamichhane, B., Westbrook, A., Cole, M.W., Braver, T.S., 2020. Exploring brain-behavior relationships in the N-back task. NeuroImage 212 (February), 116683. https://doi.org/10.1016/j.neuroimage.2020.116683.

Loeber, J.G., 2007. Neonatal screening in Europe; the situation in 2004. J. Inherit. Metab. Dis. 30, 430–438. https://doi.org/10.1007/s10545-007-0644-5.

Mencarelli, L., Neri, F., Momi, D., Menardi, A., Rossi, S., Rossi, A., Santarnecchi, E., 2019. Stimuli, presentation modality, and load-specific brain activity patterns during n-back task. Hum. Brain Mapp. 40 (13), 3810–3831. https://doi.org/10.1002/hbm.24633.

Nachev, P., Kennard, C., Husain, M., 2008. Functional role of the supplementary and pre-supplementary motor areas. Nat. Rev. Neurosci. 9 (11), 856–869. https://doi.org/10.1038/nrn2478.

Nardecchia, F., Manti, F., Chiarotti, F., Carducci, C., Carducci, C., Leuzzi, V., 2015. Neurocognitive and neuroimaging outcome of early treated young adult PKU patients: A longitudinal study. Mol. Genet. Metab. 115, 84–90. https://doi.org/10.1016/j.ymgme.2015.04.003.

Niendam, T.A., Laird, A.R., Ray, K.L., Dean, Y.M., Glahn, D.C., Carter, C.S., 2012. Meta-analytic evidence for a superordinate cognitive control network subserving diverse executive functions. Cognit., Affect. Behav. Neurosci. 12 (2), 241–268. https://doi.org/10.3758/s13415-011-0083-5.

Van Ool, J.S., Hurks, P.P.M., Snoeijen-schouwenaars, F.M., Tan, Y., Schelhaas, H.J., Klinkenberg, S., Snoeijen-schouwenaars, F.M., 2017. Accuracy of WISC-III and WAIS-IV short forms in patients with neurological disorders. Dev. Neurorehabilit. 00 (00), 1–7. https://doi.org/10.1080/17518423.2016.1277799.

Ostwald, D., Schneider, S., Bruckner, R., Horvath, L., 2019. Random field theory-based p-values: A review of the SPM implementation. ArXiv. https://doi.org/10.17605/OSF.IO/3DX9W.

Ott, T., Nieder, A., 2019. Dopamine and Cognitive Control in Prefrontal Cortex. Trend. Cognit. Sci. 23 (3), 213–234. https://doi.org/10.1016/j.tics.2018.12.006.

Owen, A.M., Mcmillan, K.M., Laird, A.R., 2005. N-Back Working Memory Paradigm: A Meta-Analysis of Normative Functional Neuroimaging Studies. Hum. Brain Mapp. 25, 46–59. https://doi.org/10.1002/hbm.20131.

Palermo, L., Geberhiwot, T., MacDonald, A., Limback, E., Hall, S.K., Romani, C., 2017. Cognitive Outcomes in Early-Treated Adults With Phenylketonuria (PKU): A Comprehensive Picture Across Domains. Neuropsychology 31 (3), 255–267. https://doi.org/10.1037/neu0000337.

Petermann, F., 2012. Wechsler Adult Intelligence Scale -, Fourth Edition. Pearson, Frankfurt, Germany.

Raichle, M.E., 2015. The Brain's Default Mode Network. Annu. Rev. Neurosci. 38, 433–447. https://doi.org/10.1146/annurev-neuro-071013-014030.

Romani, C., Manti, F., Nardecchia, F., Valentini, F., Fallarino, N., Carducci, C., Leuzzi, V., 2019. Adult cognitive outcomes in phenylketonuria: explaining causes of variability beyond average Phe levels. Orphanet J. Rare Dis. 14, 1–17. https://doi.org/10.1186/s13023-019-1225-z.

Scala, I., Riccio, M.P., Marino, M., Bravaccio, C., Parenti, G., Strisciuglio, P., 2020. Large neutral amino acids (Lnaas) supplementation improves neuropsychological performances in adult patients with phenylketonuria. Nutrients 12 (4), 1–12. https://doi.org/10.3390/nu12041092.

Spencer-Smith, M., Ritter, B.C., Mürner-Lavanchy, I., El-Koussy, M., Steinlin, M., Everts, R., 2013. Age, Sex, and Performance Influence the Visuospatial Working Memory Network in Childhood. Dev. Neuropsychol. 38 (4), 236–255. https://doi.org/10.1080/87565641.2013.784321.

Steffener, J., Brickman, A.M., Rakitin, B.C., Gazes, Y., Stern, Y., 2009. The Impact of Age-Related Changes on Working Memory Functional Activity. Brain Imag. Behav. 3 (3), 142–153. https://doi.org/10.1007/s11682-008-9056-x.

Stroup, B.M., Held, P.K., Williams, P., Clayton, M.K., Murali, S.G., Rice, G.M., Ney, D.M., 2016. Clinical relevance of the discrepancy in phenylalanine concentrations

analyzed using tandem mass spectrometry compared with ion-exchange chromatography in phenylketonuria. Mol. Genet. Metab. Rep. 6, 21–26. https://doi.org/10.1016/j.ymgmr.2016.01.001.

Sundermann, B., Garde, S., Dehghan Nayyeri, M., Weglage, J., Rau, J., Pfleiderer, B., Feldmann, R., 2020. Approaching altered inhibitory control in phenylketonuria: A functional MRI study with a Go-NoGo task in young female adults. Eur. J. Neurosci. 52 (8), 3951–3962. https://doi.org/10.1111/ejn.14738.

Sundermann, B., Pfleiderer, B., Möller, H.E., Schwindt, W., Weglage, J., Lepsien, J., Feldmann, R., 2011. Tackling frontal lobe–related functions in PKU through functional brain imaging: a Stroop task in adult patients. J. Inherit. Metab. Dis. 34 (3), 711–721. https://doi.org/10.1007/s10545-011-9318-4.

Surtees, R.R., Blau, N., 2000. The neurochemistry of phenylketonuria. Eur. J. Pediatr. 159, S109–S113.

Trepp, R., Muri, R., Abgottspon, S., Bosanska, L., Hochuli, M., Slotboom, J., Everts, R., 2020. Impact of phenylalanine on cognitive, cerebral, and neurometabolic parameters in adult patients with phenylketonuria (the PICO study): a randomized, placebo- controlled, crossover, noninferiority trial. Trials 21 (178), 1–11.

Tzourio-Mazoyer, N., Landeau, B., Papathanassiou, D., Crivello, F., Etard, O., Delcroix, N., Joliot, M., 2002. Automated Anatomical Labeling of Activations in SPM Using a Macroscopic Anatomical Parcellation of the MNI MRI Single-Subject Brain. NeuroImage 15 (1), 273–289. https://doi.org/10.1006/nimg.2001.0978.

Van Snellenberg, J.X., Slifstein, M., Read, C., Weber, J., Thompson, J.L., Wager, T.D., Smith, E.E., 2015. Dynamic Shifts in Brain Network Activation During Supracapacity Working Memory Task Performance. Hum. Brain Mapp. 36 (4), 1245–1264. https://doi.org/10.1002/hbm.22699.

Van Spronsen, F.J., Hoeksma, M., Reijngoud, D.-J., 2009. Brain dysfunction in phenylketonuria. Metab. Dis. 32, 46–51. https://doi.org/10.1007/s10545-008-0946-2.

Van Vliet, D., Van Wegberg, A.M.J., Ahring, K., Bik-Multanowski, M., Blau, N., Bulut, F. D., Van Spronsen, F.J., 2018. Can untreated PKU patients escape from intellectual disability? A systematic review. Orphanet Journal of Rare Diseases 13 (1), 1–6. https://doi.org/10.1186/s13023-018-0890-7.

van Vliet, D., van Wegberg, A.M.J., Ahring, K., Bik-Multanowski, M., Casas, K., Didycz, B., van Spronsen, F.J., 2019. Untreated PKU Patients without Intellectual Disability: What Do They Teach Us? Nutrients 11, 1–10. https://doi.org/10.3390/nu11112572.

Van Wegberg, A.M.J., MacDonald, A., Ahring, K., Bélanger-Quintana, A., Blau, N., Bosch, A.M., van Spronsen, F.J., 2017. The complete European guidelines on phenylketonuria: diagnosis and treatment. Orphanet J. Rare Dis. 12 (1), 162. https://doi.org/10.1186/s13023-017-0685-2.

Waisbren, S. E., Prabhu, S. P., Anastasoaie, V., Charette, K., Rodriguez, D., Merugumala, S., & Lin, A. P. (2016). Improved Measurement of Brain Phenylalanine and Tyrosine Related to Neuropsychological Functioning in Phenylketonuria. Doi: 10.1007/8904.

White, D. A., Nortz, M. J., Mandernach, T., Huntington, K., & Steiner, R. D. (2002). Age-related working memory impairments in children with prefrontal dysfunction associated with phenylketonuria, 1–11.

Yarkoni, T., Poldrack, R.A., Nichols, T.E., Van Essen, D.C., Wager, T.D., 2011. Large-scale automated synthesis of human functional neuroimaging data. Nat. Methods 8 (8), 665–670. https://doi.org/10.1038/nmeth.1635.

Zhu, W., Zeng, N., Wang, N., 2010. Sensitivity, Specificity, Accuracy, Associated Confidence Interval and ROC Analysis with Practical SAS ® Implementations. Proceedings Nesug. 2010, 1–9.